GEOLOGICA CARPATHICA, 55, 6, BRATISLAVA, DECEMBER 2004
487–500

GEOCHEMISTRY OF POST-COLLISION PLIOCENE-QUATERNARY KARASAR BASALT (DİVRİĞİ-SİVAS, EASTERN TURKEY): EVIDENCE FOR PARTIAL MELTING PROCESSES

MUSA ALPASLAN[1], HÜSEYİN YILMAZ[2] and ABİDİN TEMEL[3]

[1]Mersin Üniversity, Department of Geology, 33343 Mersin, Turkey; malpaslan@mersin.edu.tr; musaalp@yahoo.com
[2]Cumhuriyet University, Department of Geophysics, 58140 Sivas, Turkey
[3]Hacettepe University, Department of Geology, 06532 Beytepe-Ankara, Turkey

(Manuscript received February 5, 2003; accepted in revised form December 16, 2003)

Abstract: The Pliocene-Quaternary Karasar basalt is located in the western part of the post-collisional volcanic field in Eastern Anatolia and occurs as lava flows on the continental sediments. According to normative mineralogy and geochemistry, Karasar basalt samples have hyperstene-normative tholeiites, nepheline-normative basalts, trachybasalts, and basaltic andesites with quartz-xenocrysts which occur at the base of the lava flows. Trace and rare element variations indicate that the trachybasalts are enriched in highly incompatible trace and light-rare earth elements relative to hyperstene- and nepheline-normative basalts. Hy-normative tholeiites have higher concentrations of medium-heavy rare earth elements relative to ne-normative basalts and trachybasalts. The trace element characteristics of the Karasar basalt imply that the quartz-bearing rocks indicate some crustal contributions, but the basaltic samples have a minimal or no crustal assimilation. Th/Yb-Nb/Yb and Hf/Sm_N-Ta/La_N diagrams coupled with HFSE depletions display a subduction signature in the source region of these volcanics. REE modeling exhibits that the magmas forming the Karasar basalt originated from a spinel-peridotite source, although trachybasalts require mixing between melts from spinel- and garnet-peridotite source. Discrimination plots based on trace element data exhibit a within-plate character of the Karasar basalts. Correlations between trace element ratios (Ba/Nb-La/Nb and Ba/La-Ce/Pb) imply that the source of Karasar basalt is lithospheric rather than the asthenospheric mantle. These data reveal that the Karasar basalt is linked to a post-collisional extensional tectonic regime following the collision between the Eurasian and Arabian plates. Volcanism in this part of Anatolia is consistent with a model in which melting of lithospheric mantle occurred in response to lithospheric extension.

Key words: Eastern Anatolia, within-plate, extensional, post-collision, alkaline, tholeiitic, petrology.

Introduction

Intracontinental basaltic volcanism provides samples which can be used to investigate mantle compositions and crustal assimilations, and numerous studies have documented evidence for crustal assimilations and compositional heterogeneities on a range of scales (Hart 1984; McDunough et al. 1985; Zindler & Hart 1986; McDunough 1990; Saunders et al. 1992; White & McKenzie 1995; Turner & Hawkesworth 1995; Saunders et al. 1998; Reiners 2002). Studies of these basalts suggest that the compositions of the intracontinental basalts are similar to ocean-island basalts (OIB), which are suggested to be generated in the convecting mantle (Wilson 1989, 1993; White & McKenzie 1995). These melts are often compositionally modified during ascent from asthenospheric mantle including partial melting, fractionation, contamination of crustal rocks and magma mixing (Hawkesworth et al. 1984; Wooden et al. 1993; Turner & Hawkesworth 1995). Crustal contamination of mantle-derived magmas has also been invoked to account for trace element signatures (Arndt & Christensen 1992; Arndt et al. 1993; Wooden et al. 1993; Baker et al. 1997; Fram & Lesher 1997). Identification of mantle source and evolution processes of primary magmas of the intracontinental basalts have been a major goal of the studies concerned with many continental basaltic provinces (Hawkesworth et al. 1979; Heming 1980; McDunough et al. 1985; Weaver 1991; Coffin & Eldholm 1992; Saunders et al. 1992, 1998).

Geodynamic models suggest that the Anatolian plate was deformed as a result of the collision of the Eurasian and Arabian plates along the Bitlis Suture Zone (McKenzie 1972; Şengör 1980). This collision, which initiated the Neotectonic period, resulted in the shortening of Eastern Anatolia (McKenzie 1972; Şengör & Kidd 1979; Şengör et al. 1985). Convergence between the Eurasian and Arabian plates along the Bitlis Suture Zone caused a compressional–contractional tectonic regime at the end of late Miocene and late early Pliocene (Koçyiğit et al. 2001). In late early Pliocene, three major neotectonic structures, the North Anatolian and East Anatolian Transform Faults and the Anatolian plate, formed and the Anatolian plate commenced to escape in a WSW direction onto the oceanic lithosphere of the African plate (Hempton 1987). Thus, an earlier compressional–contractional tectonic regime was replaced by a compressional–extensional tectonic regime at the late early Pliocene, with extrusion tectonics dominated by strike-slip faulting (Koçyiğit et al. 2001).

Extensive volcanic activity took place in Eastern Anatolia during the neotectonic period, as a result of which volcanic rocks covered large areas of Eastern Anatolia. A number of researchers discussed the origin, age and tectonic settings of the post-collisional volcanic rocks in the Eastern Anatolia (Lambert et al. 1974; Innocenti et al. 1976; Şaroğlu & Yılmaz 1984;

Gülen 1984; Tokel 1984; Alpaslan & Terzioğlu 1996; Keskin et al. 1998; Yılmaz et al. 1998; Buket & Temel 1998; Fig. 1) and suggested that the alkaline volcanics closely related to the extentional regime during Neogene period (Pearce et al. 1990; Yılmaz et al. 1998).

The objective of this study is to explain the origin and processes that determined the geochemical characteristics of the Karasar basalt in the western part of Eastern Anatolia.

Geological setting

The study area is located in the Central–Eastern Anatolia (east of Sivas, Fig. 1) and is a part of the region, which is under approximately north-south and NNE–SSW shortening related to the collisional processes between the Anatolian and Arabian plates along the Bitlis Suture Zone (Bozkurt 2001). As a result of the collision between the Arabian and Anatolian plates, the eastern part of Anatolia has experienced an intracontinental convergence (McKenzie 1969) that resulted in crustal thickening and uplift (Şengör & Kidd 1979) and collision related volcanics indicated by 12–15 Ma calc-alkaline Yamadağı volcanics in the study area (Fig. 2; Yılmaz et al. 1998; Ekici 2003). Following the continental collision, the earlier compressional tectonic regime was replaced by a new compressional–extensional tectonic regime by the early Pliocene (Koçyiğit et al. 2001). This has resulted in the generation of intra-continental strike-slip faults namely the North Anatolian and East Anatolian Fault Zones (Fig. 1). The formation of these fault zones and subsequent westward escape of the Anatolian plate along its boundary structures has resulted in the generation of the Central Anatolian Ova Province in the eastern parts of the Anatolian plate (Şengör & Yılmaz 1981). The structural elements of the study area affecting Neogene units have been dominated by second order NW–SE left and NE–SW right lateral strike-slip faults (Fig. 2) which may be accompanied by North Anatolian and East Anatolian faults. Basaltic volcanics outcropping as thick lava flows, namely the Karasar basalt, postdates 12–15 Ma collision-related Yamadağı volcanics (Ekici 2003) and overlie the basic pyroclastics and continental sediments named the İnallı Formation (Gültekin 1993; Figs. 2, 3).

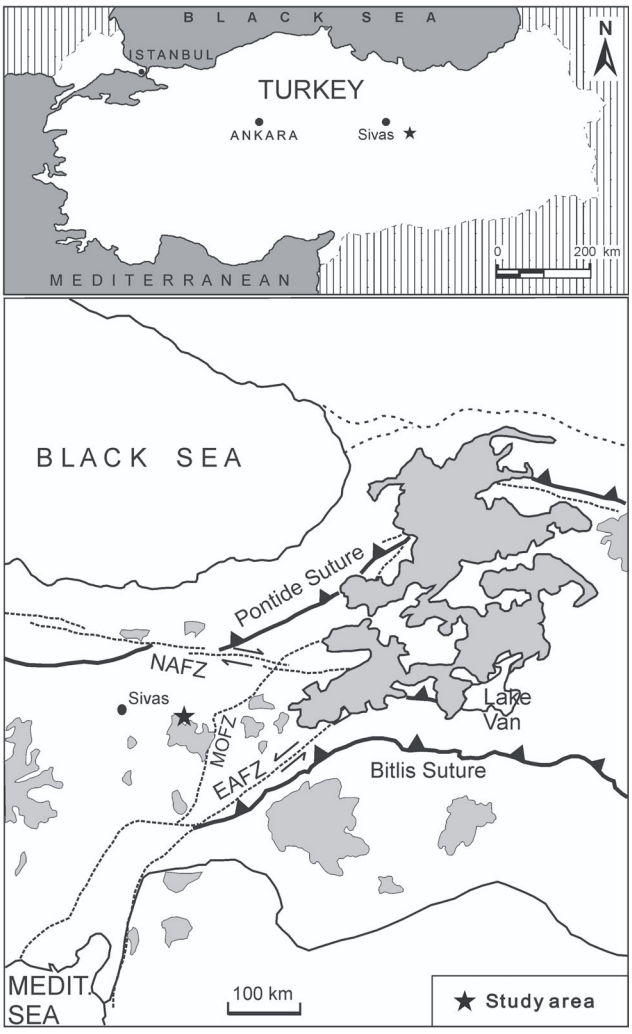

Fig. 1. Location map of the study area and distribution of the Neogene volcanics in Eastern Turkey (simplified from Pearce et al. 1990).

Petrography

The Karasar basalt is mainly dominated by hyperstene-normative and nepheline-normative basalts and trachybasalts (hawaiite) (Fig. 4 and Table 1) but quartz-xenocrysts-bearing rocks found at the base of the volcanic sequence have been obtained from drilling core samples.

Xenocryst-bearing rocks have strongly prophyrytic texture and include olivine and plagioclase phenocrysts. Quartz xenocrysts are surrounded by a reaction rim with clinopyroxene microlithes. Olivines are iddingsitizated. Plagioclases occur as sieve-textured phenocrysts and microlithes. The groundmass of these samples consists of volcanic glass, clinopyroxene and plagioclase microlithes, and scarce opaque minerals. These rocks fall into the basaltic andesite field in the total alkali-silica nomenclature diagram (Fig. 4) of the Le Maitre (1989).

Samples which fall on the basalt field of the nomenclature diagram (Fig. 4) have a holocrystalline-intersertal texture. Their normative mineralogies indicate that these samples are hyperstene-normative and nepheline-normative basalts. The mineral assemblages of these rocks are olivine, clinopyroxene, plagioclase and minor opaque minerals. The euhedral and subhedral olivines occur as phenocrysts and microphenocrysts. They are generally serpentinitizated and also iddingsitizated in some rock samples. The plagioclases have commonly been seen as microlithes which are perpendicular to each other. The clinopyroxenes are generally subhedral and fill the areas between the plagioclases laths.

Trachybasalts (hawaiite) occur as last flows in the study area. They are characterized by fine-grained and aphanitic texture. These rocks have a holocrystalline-intersertal texture under the microscopy and include olivine, clinopyroxene, plagioclase, and minor opaque minerals. Olivines occur as euhedral and subhedral shaped phenocrysts and microphenocrysts, and are iddingsitizated. They also occur in glomerophy-

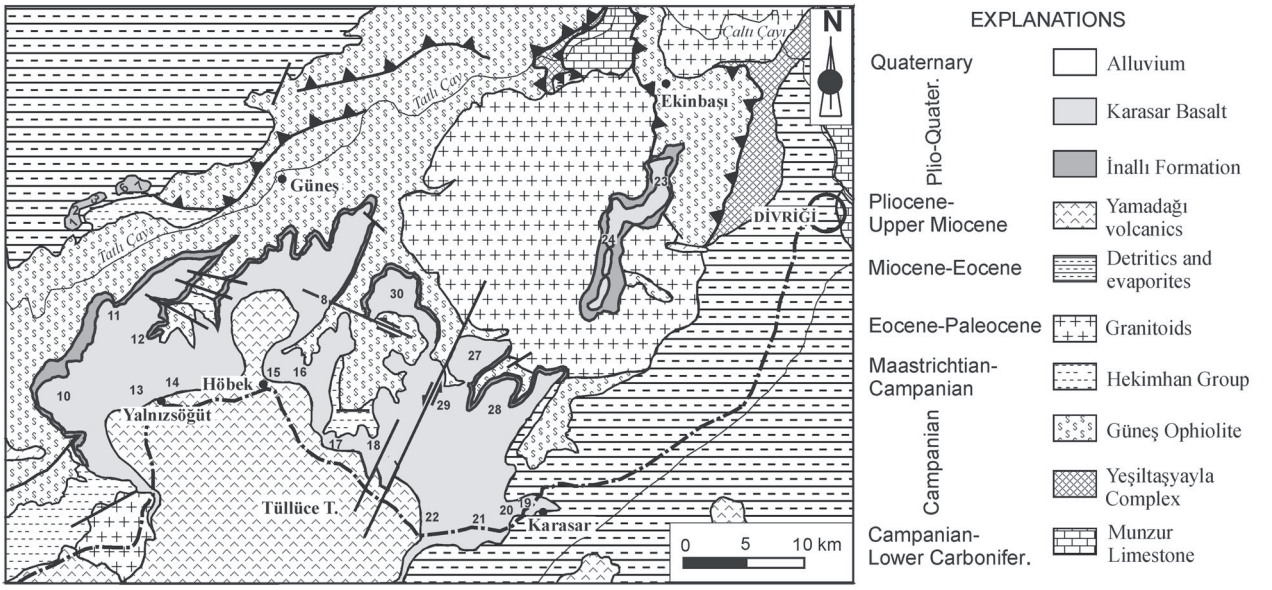

Fig. 2. Simplified geological map of the study area.

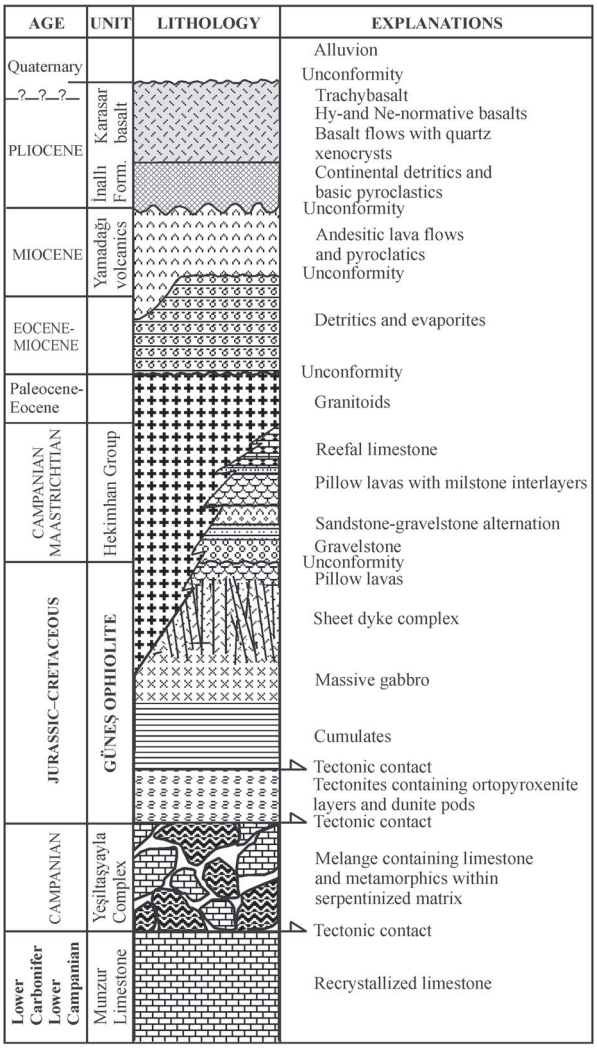

Fig. 3. Generalized tectonostratigraphical columnar section of the study area.

ric aggregates. Plagioclases have been seen as microlithes which are perpendicular to each other. Clinopyroxenes are generally subhedral.

Carbonates and zeolites can be seen as secondary minerals in the rock samples of all the lava flows.

Analytical techniques

Twenty-seven samples of the Karasar basalt were analysed for major and twenty-six samples for trace element concentrations (Table 1). For major-element analyses, fused disks were prepared by using six parts of prepared flux (lithium tetraborate) and one part of rock powder. The mixtures were fused in crucibles of 95 % Pt and 5 % Au at 1050 °C for 60 minutes to form a homogeneous melt. The melt was then poured into a preheated mold to chill to a thick glass disk. Whole rock analyses were performed at Hacettepe University using PHILIPS PW 1480 X-ray spectrometer. Trace element and rare element concentrations of 17 samples were analysed at ACME laboratories (Canada) by ICP-MS using fusion method.

Geochemistry

Representative geochemical data and normative mineralogy are listed in Table 1. Figure 5 exhibits that the xenocryst bearing rocks plot in subalkaline field. These rocks will not be shown in geochemical interpretative diagrams because of their quartz-xenocryst contents. Samples seen in basalt field in Fig. 4 fall into both the alkaline and subalkaline fields. On the basis of normative mineralogy, these rocks can be named as hyperstene-normative tholeiites and nepheline-normative basalts (Table 1). Trachybasalts have an alkaline character in Fig. 5. Selected elements are illustrated in Fig. 6. Trachybasalts are characterized by high TiO_2, P_2O_5, K_2O and Na_2O and incompatible elements such as Rb, Nb and Zr. Nepheline-nor-

Table 1: Geochemical analyses results of the Karasar basalt. (Total iron as Fe_2O_3, LOI as loss on ignition, major oxides and trace and rare earth elements as per cent and ppm, respectively.)

	m1	m2	m3	m3a	m6	m7	m8	m9	m10	m11	m12
SiO_2	46.52	46.32	47.64	45.47	47.41	47.80	46.00	48.84	49.10	48.09	45.22
TiO_2	1.28	1.32	1.42	1.30	1.36	1.34	1.34	1.55	1.53	1.34	1.24
Al_2O_3	16.06	15.93	16.39	16.25	16.76	17.07	16.65	16.94	17.18	17.23	16.02
Fe_2O_3	10.70	10.80	11.11	10.05	10.38	10.46	10.26	11.02	10.90	11.14	10.37
MnO	0.16	0.16	0.17	0.15	0.16	0.16	0.16	0.16	0.16	0.17	0.15
MgO	7.59	7.60	7.66	4.15	4.85	4.41	5.19	4.89	4.82	4.49	4.87
CaO	8.99	8.86	8.73	12.86	11.16	10.87	11.55	9.55	9.56	9.93	12.97
Na_2O	2.79	2.84	3.17	3.22	3.41	3.45	3.40	3.53	3.55	3.38	3.10
K_2O	0.74	0.69	0.51	0.54	0.55	0.56	0.55	0.76	0.76	0.57	0.51
P_2O_5	0.19	0.18	0.20	0.19	0.19	0.19	0.18	0.28	0.28	0.20	0.18
LOI	4.05	4.43	2.76	4.88	3.30	3.42	3.87	2.45	2.36	2.93	4.53
Total	99.07	99.13	99.76	99.06	99.53	99.72	99.15	99.47	100.2	99.47	99.16
Normative Mineralogy											
Q	–	–	–	–	–	–	–	–	–	–	–
Or	4.61	4.31	3.11	3.39	3.38	3.43	3.41	4.63	4.60	3.49	3.19
Ab	24.84	25.37	27.65	18.84	26.62	30.29	21.74	30.63	30.70	29.62	16.98
An	30.67	30.31	29.91	30.06	29.95	30.57	29.98	28.87	29.36	31.27	29.92
Ne	–	–	–	5.47	1.82	–	4.58	–	–	–	5.82
Di	12.39	12.31	11.13	30.33	21.88	19.80	24.02	14.93	14.45	15.46	30.63
Hy	6.90	6.58	7.20	–	–	0.57	–	4.41	4.98	4.66	–
Ol	14.38	14.79	14.49	5.79	10.13	7.25	10.11	9.65	9.12	9.09	7.43
Mag	3.26	3.31	3.32	3.09	3.13	4.19	3.12	3.28	3.23	3.35	3.18
Il	2.56	2.65	2.78	2.62	2.68	2.64	2.67	3.02	2.97	2.64	2.49
Ap	0.47	0.45	0.49	0.48	0.47	0.46	0.45	0.68	0.68	0.49	0.45
Pb	2.50	3.30	2.60	2.10	2.80	2.90	2.20	3.20	3.00	2.80	2.40
V	187	183	205	181	179	181	184	200	195	219	174
Rb	12.7	13.5	12.2	10.2	10.5	11.1	11.8	15.6	14.7	11.6	8.9
Cs	0.30	0.40	0.50	0.10	0.10	0.10	0.60	0.30	0.30	0.10	0.10
Ba	126.5	113.9	132.6	178.5	145.2	165	303.1	227.3	235.5	262.6	329.2
Sr	508	516.4	552	353.8	351.4	355.6	344.3	391.1	387.9	346.9	333.5
Ga	16	17	17	17	16	17	18	16	17	18	17
Ta	0.50	0.40	0.52	0.40	0.40	0.40	0.40	0.70	0.70	0.50	0.40
Nb	5.2	5.3	5.2	6.1	6.0	6.0	6.1	8.8	8.4	6.1	5.4
Hf	2.70	2.90	3.40	2.90	2.80	2.70	3.20	3.90	3.70	2.80	2.90
Zr	109	111	119	110	113	111	113	136	136	117	111
Y	26.6	26.9	30.8	25.1	27.9	26.2	27	27.8	26.7	28.5	26.7
Th	1.80	3.00	2.50	2.1	2.2	2.3	2.8	3.5	3.3	2.4	3.4
U	0.4	0.8	0.8	0.2	0.3	0.4	0.3	0.6	0.3	0.7	0.3
La	10.9	11.0	11.7	10.7	11.0	10.4	11.0	15.7	15.9	12.1	10.9
Ce	21.6	23.0	25.0	24	24.1	22.8	24.3	30.9	31.8	25.8	23.6
Pr	2.90	2.94	3.14	3.06	2.97	2.97	3.11	3.97	3.89	3.22	2.97
Nd	12.3	12.8	13.3	14.0	14.7	13.7	14.3	16.3	17.8	13.5	13.6
Sm	3.8	3.4	3.6	3.3	3.6	3.6	3.2	4.5	4.5	3.7	3.0
Eu	1.17	1.15	1.26	1.34	1.23	1.26	1.26	1.38	1.36	1.19	1.19
Gd	3.86	3.95	4.34	4.06	4.15	4.01	3.97	4.61	4.17	4.21	3.84
Tb	0.68	0.72	0.72	0.72	0.78	0.75	0.76	0.79	0.69	0.72	0.72
Dy	4.43	4.63	5.05	4.36	4.73	4.00	4.43	4.72	4.33	4.65	3.97
Ho	0.94	0.93	1.03	0.89	0.96	0.94	0.88	0.97	0.98	0.95	0.95
Er	2.74	2.93	3.04	2.47	2.64	2.55	2.69	2.71	2.75	2.87	2.53
Tm	0.39	0.45	0.46	0.38	0.43	0.41	0.43	0.41	0.40	0.43	0.36
Yb	2.40	2.75	3.00	2.79	2.34	2.66	2.53	2.90	2.57	2.71	2.55
Lu	0.42	0.43	0.47	0.37	0.39	0.41	0.41	0.45	0.39	0.42	0.39
Zr/Nb	20.86	20.84	22.92	17.96	18.76	18.51	18.57	15.47	16.19	19.22	20.53
Zr/Y	4.07	4.10	3.87	4.36	4.02	4.24	4.19	4.89	5.09	4.11	4.15
Ba/Nb	24.32	21.49	25.50	29.26	24.20	27.5	49.68	25.82	28.03	43.04	60.96
Ba/La	11.02	9.80	10.99	16.68	13.20	15.86	27.55	14.11	14.49	20.95	30.20
$(La/Sm)_N$	1.85	2.09	2.10	2.09	1.97	1.86	2.22	2.25	2.28	2.11	2.27

mative and hyperstene-normative basalts generally overlap with each other, although hyperstene-normative tholeiites have relatively high contents of Fe_2O_3, MgO and V (Fig. 6). Primitive mantle-normalized La/Sm ratios [$(La/Sm)_N$] of the Karasar basalt range between 1.85 and 3.33 (Table 1). Trachybasalts have high $(La/Sm)_N$ ranging between 2.99 and 3.33, whereas tholeiites 1.85–2.57 and nepheline-normative basalts 1.86–2.67. Trachybasalts (hawaiite) have higher TiO_2, K_2O, Na_2O, P_2O_5 and Zr contents with correspondingly higher LREE (La = 27.08–22.91 ppm) contents relative to hyperstene-normative tholeiites (19.96–11.47) and nepheline-normative basalts (10.70–15.30) and more fractionated REE patterns. La/Yb_N ratios vary between 6.19 and 8.48 for trachybasalts (hawaiite), 4.90 and 2.80 for hy-normative basalts and 4.28–2.75 for ne-normative basalts, whereas Gd/Yb_N ratios vary between 1.46 and 1.87 for trachybasalts (hawaiite), 1.62 and 1.19 for hy-normative basalts, and 1.47 and 1.20 for ne-normative basalts. The LILE (large-ion lithophile elements, e.g. K, Rb, Ba, Sr) and HFSE (high-field strength elements; Nb, Th, U, Ta) are also relatively co-enriched along with LREE in the trachybasalts compared to nepheline-normative basalt and hyperstene-normative tholeiites (Table 1).

Table 1: *Continuing.*

	m13	m14	m15	m16	m17	m18	m19	m20	m21	m22	m23
SiO_2	47.09	48.59	48.91	48.52	54.42	54.99	50.30	50.71	54.34	55.07	49.44
TiO_2	1.41	1.54	1.29	1.34	1.16	1.13	1.73	1.67	1.15	1.14	1.75
Al_2O_3	16.60	16.75	17.62	17.00	16.17	16.24	15.96	15.93	16.31	16.30	16.31
Fe_2O_3	10.41	11.04	10.59	10.57	8.48	8.27	10.03	9.86	8.38	8.34	10.45
MnO	0.15	0.16	0.21	0.19	0.14	0.12	0.14	0.14	0.14	0.13	0.15
MgO	4.71	5.62	5.33	5.91	4.94	4.50	6.36	5.23	4.82	4.85	4.64
CaO	11.18	9.50	9.70	9.97	7.71	7.53	6.96	7.18	7.80	7.47	8.16
Na_2O	3.34	3.46	3.50	3.51	3.60	3.75	3.97	4.05	3.74	3.70	4.05
K_2O	0.69	0.74	0.52	0.54	1.11	1.18	1.31	1.38	1.13	1.20	1.19
P_2O_5	0.26	0.29	0.19	0.18	0.17	0.19	0.37	0.38	0.17	0.18	0.34
LOI	3.42	2.48	2.55	2.03	2.21	1.88	2.04	2.40	2.16	2.27	2.61
Total	99.29	100.17	100.41	99.76	100.1	99.78	100.17	99.93	100.14	100.38	99.10
Normative mineralogy											
Q	–	–	–	–	5.96	6.53	–	–	5.18	6.24	–
Or	4.26	4.49	3.14	3.27	6.68	7.15	7.98	8.45	6.80	7.21	7.27
Ab	25.71	29.97	30.26	30.39	31.14	32.41	34.61	35.54	32.32	31.82	35.54
An	29.51	28.69	31.53	29.73	13.25	24.50	22.48	21.95	24.89	24.73	23.63
Ne	2.05	–	–	–	–	–	–	–	–	–	–
Di	22.17	14.77	13.67	16.33	10.32	10.05	8.53	10.03	10.91	9.49	13.06
Hy	–	3.48	4.84	0.29	13.56	12.33	12.05	13.22	12.81	13.46	5.56
Ol	9.80	11.75	10.52	13.87	–	–	4.64	1.24	–	–	5.15
Mag	3.15	3.28	3.13	3.15	3.89	3.84	4.76	4.68	3.87	3.86	4.80
Il	2.79	2.99	2.50	2.60	2.24	2.18	3.38	3.29	2.22	2.20	3.44
Ap	0.64	0.71	0.46	0.44	0.39	0.44	0.88	0.90	0.39	0.42	0.81
Pb	2.80	2.60	1.90	3.80	1.80	2.70	1.40	1.40	1.80	7.90	4.90
V	192	222	209	210	152	148	151	159	157	148	143
Rb	13.7	18	10.5	11.9	37.1	36.9	33.2	35.6	32.7	32.5	22.6
Cs	0.10	0.50	0.10	0.10	2.40	2.20	1.20	0.70	1.80	1.60	0.30
Ba	222.9	566.1	237.2	225.2	222.5	240.3	273.8	289	215	233.4	217.4
Sr	416.3	403.9	371.6	360.8	353.7	362.4	536.2	568.9	360.6	355.2	529.3
Ga	17	17	17	18	18	17	17	18	17	18	18
Ta	0.60	0.60	0.40	0.50	0.60	0.50	1.0	1.0	0.40	0.30	0.60
Nb	8.4	9.2	6.4	5.8	7.1	7.0	15.4	15.6	7.5	7.1	13.2
Hf*	2.60	3.40	2.90	2.50	3.90	3.50	4.80	4.90	3.30	3.10	4.60
Zr	131	144	117	117	128	129	197	206	127	132	171
Y	28.6	30.2	27.5	27	24.3	24.2	25.9	24.9	23.1	25.7	28.7
Th	3.6	3.3	1.9	2.5	6.2	6.8	7.2	7.1	7.4	6.6	4.7
U	0.5	0.8	0.5	0.7	2.3	2.1	1.4	2.2	2.1	2.2	0.3
La	15.3	19.5	11.6	11.3	16.7	17.8	26.3	26.5	26.1	19.3	22.1
Ce	33.0	34.9	22.9	23.1	31.7	31.5	51.3	53.1	32.0	34.3	41.8
Pr	3.98	4.54	3.12	3.02	3.56	3.68	5.79	5.85	3.56	4.10	4.78
Nd	18.6	18.8	12.7	14.1	14.8	15.0	24.1	22.1	14.4	16.4	20.5
Sm	3.7	4.9	3.4	3.5	3.5	3.7	5.1	5.6	3.2	4.7	4.5
Eu	1.36	1.43	1.24	1.19	1.17	1.18	1.65	1.60	1.11	1.25	1.55
Gd	4.49	5.12	3.63	4.08	4.06	4.04	4.81	5.06	3.61	4.19	4.51
Tb	0.73	0.80	0.69	0.69	0.63	0.57	0.77	0.82	0.60	0.76	0.75
Dy	4.52	5.12	4.54	4.76	4.11	3.79	5.05	4.49	4.03	4.36	4.56
Ho	0.91	1.05	0.97	0.93	0.78	0.77	0.88	0.90	0.82	0.85	0.88
Er	2.50	3.01	3.00	2.80	2.36	2.41	2.68	2.41	2.44	2.56	2.72
Tm	0.42	0.43	0.44	0.42	0.35	0.32	0.35	0.33	0.37	0.35	0.35
Yb	2.56	2.85	2.68	2.60	2.07	2.30	2.41	2.24	2.51	2.60	2.56
Lu	0.37	0.41	0.38	0.41	0.34	0.36	0.39	0.36	0.33	0.37	0.35
Zr/Nb	15.57	15.60	18.20	20.10	18.08	18.40	12.77	12.89	17.13	18.54	12.97
Zr/Y	4.55	4.75	4.23	4.31	5.28	5.32	7.59	7.28	5.56	5.12	5.96
Ba/Nb	26.53	61.51	37.06	38.82	31.33	34.32	17.77	18.06	28.66	32.87	16.46
Ba/La	14.56	28.35	20.01	19.47	13.04	13.21	10.11	10.52	13.08	11.89	9.49
$(La/Sm)_N$	2.67	2.57	2.20	2.08	3.08	3.10	3.33	3.05	3.25	2.65	3.17

On a primitive mantle normalized trace element diagram indicate that all types of the Karasar basalt have parallel patterns to each other (Fig. 7a). Trachybasalts have higher concentrations of more incompatible elements than those of nepheline-normative basalt and hyperstene-normative tholeiites, although hyperstene-normative tholeiites have higher concentrations of less incompatible elements such as Y and Yb, than those of other basalts (Fig. 7a). Decreases of greater magnitude from trachybasalt to nepheline-normative and hyperstene-normative basalts are generally associated with more incompatible elements (e.g. La, Rb, K), so that ratios of highly to moderately incompatible elements show similar decreases in the same manner. All other incompatible elements (e.g. K_2O, Na_2O and P_2O_5) show a decrease from trachybasals to others. All samples display marked, but variable, depletions in Nb and Ta. A Nb-Ta trough is a common feature in continental flood basalts. This signature also resembles that of volcanic arc basalts. Furthermore, negative Nb and Ta anomalies could also result from crustal contamination of magmas (Winter 2001).

Primitive mantle normalized rare earth element (REE) profiles of the Karasar basalt are shown in Fig. 7b. Figure 7b

Table 1: *Continuing.*

	m24	m27	m28	m29	m30
SiO_2	49.89	45.21	45.08	48.89	46.39
TiO_2	1.80	1.35	1.43	1.43	1.45
Al_2O_3	16.55	16.45	15.79	16.65	16.53
Fe_2O_3	10.64	9.96	9.95	10.39	10.32
MnO	0.15	0.14	0.15	0.15	0.14
MgO	4.43	3.10	4.89	5.37	3.98
CaO	7.73	13.13	12.37	9.16	11.35
Na_2O	4.17	3.30	3.23	3.12	3.50
K_2O	1.22	0.64	0.65	0.65	0.70
P_2O_5	0.35	0.23	0.23	0.23	0.24
LOI	2.29	5.49	4.79	2.99	3.99
Total	99.22	99.10	98.56	99.03	98.59
Normative mineralogy					
Q	–	–	–	–	–
Or	7.65	4.05	4.10	4.01	4.38
Ab	36.39	18.23	18.45	27.49	24.52
An	23.55	30.16	28.45	30.74	28.90
Ne	–	6.30	5.79	–	3.68
Di	11.11	31.91	29.18	12.50	24.24
Hy	7.50	–	–	16.26	–
Ol	4.00	3.03	7.49	2.52	7.68
Mag	4.87	3.09	3.07	3.15	3.16
Il	3.53	2.74	2.90	2.83	2.91
Ap	0.83	0.58	0.58	0.57	0.60
Pb	5.80	3.20	–	2.20	3.40
V	150	194	–	198	206
Rb	25.2	15.6	–	18.4	17.9
Cs	0.30	0.40	–	1.20	0.50
Ba	221.6	206.1	–	135.6	166
Sr	530.6	387	–	371.1	402.7
Ga	17	17	–	17	18
Ta	1.50	0.5	–	5.90	0.50
Nb	14.7	7.4	–	7.5	7.6
Hf	4.20	2.90	–	2.90	3.20
Zr	182	127	–	119	135
Y	29.4	27.6	–	24.9	28.4
Th	5.9	3.1	–	3.3	3.4
U	0.6	0.3	–	0.5	0.5
La	23.2	13.3	–	13.2	10.4
Ce	43.9	28.8	–	28.6	29.7
Pr	5.13	3.58	–	3.29	3.66
Nd	20.6	17.7	–	14.3	18.9
Sm	5.0	3.6	–	4.1	3.8
Eu	1.58	1.37	–	1.25	1.43
Gd	4.90	4.29	–	4.02	4.46
Tb	0.80	0.72	–	0.67	0.85
Dy	4.90	4.96	–	4.52	4.35
Ho	0.91	0.97	–	0.83	1.01
Er	2.53	2.63	–	2.54	2.73
Tm	0.39	0.41	–	0.36	0.41
Yb	2.58	2.52	–	2.73	2.77
Lu	0.40	0.42	–	0.34	0.41
Zr/Nb	12.36	17.21	–	15.82	17.78
Zr/Y	6.18	4.61	–	4.76	4.76
Ba/Nb	15.07	27.85	–	18.08	21.84
Ba/La	9.25	15.49	–	9.86	11.77
$(La/Sm)_N$	2.99	2.38	–	2.08	2.33

shows that the trachybasalt has a steeper slope in light rare element (LREE) contents than the hy-normative tholeiites and nepheline-normative basalts, whereas the hy-normative tholeiites have higher concentrations of HREE (Fig. 7b). LREE patterns exhibit a characteristic feature that there is a decrease from trachybasalt to nepheline-normative and hyperstene-normative basalts, although hyperstene-normative tholeiitic basalts have higher heavy rare earth element (HREE) contents relative to others.

Discrimination plots (Fig. 8) based on trace element data show that the Karasar basalt was derived from the melts generated in a within-plate environment.

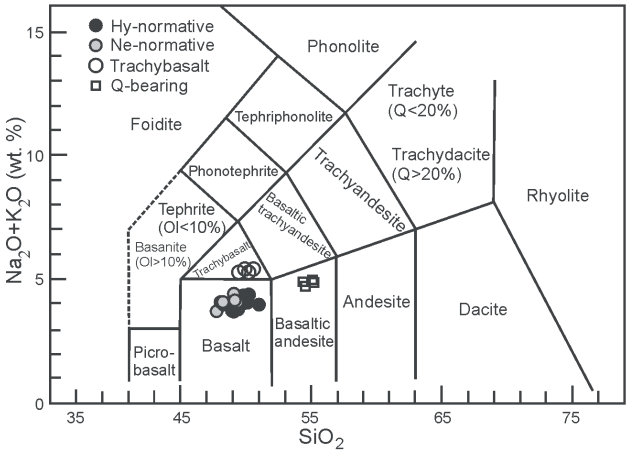

Fig. 4. Total alkali-silica nomenclature diagram (LeMaitre 1989) for the Karasar basalt. Black circles — hy-normative tholeiites, grey-circles — ne-normative basalts, open circles — trachybasalts, open squares: samples with quartz xenocrysts.

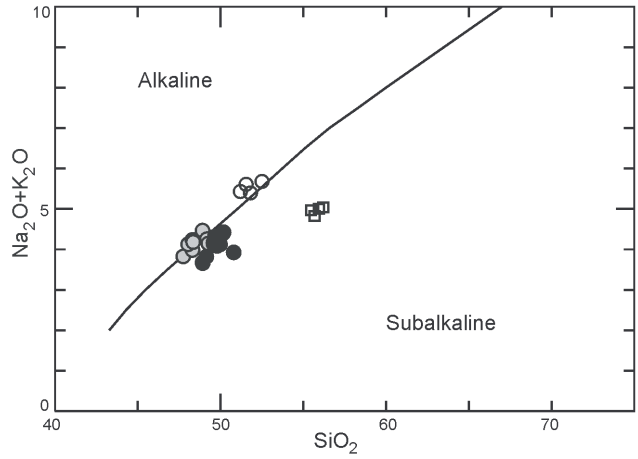

Fig. 5. Total alkali-silica diagram of Irvine & Baragar (1971) showing that the Karasar basalt falls into the alkaline field, but samples containing quartz xenocrysts fall in the subalkaline field. (Symbols as in Fig. 4.)

Discussion

In this study, the petrogenetic features of both types of the Karasar basalt have been determined using trace and rare earth element geochemistry. Differences in the incompatible trace and rare element contents of the Karasar basalt can be explained by fractionation, crustal contamination, source characteristics and varying degrees of partial melting in a source material. These will be discussed below.

Fractional crystallization

Although Karasar basalt samples do not satisfy the compositional criteria for identifying primary upper mantle partial melts because of their Mg-numbers <63 %, the effects of fractional crystallization in the evolution of the Karasar basalt lavas are suggested by the geochemical data (Fig. 6). MgO contents ranging from 7.66 to 3.10 may suggest crystal

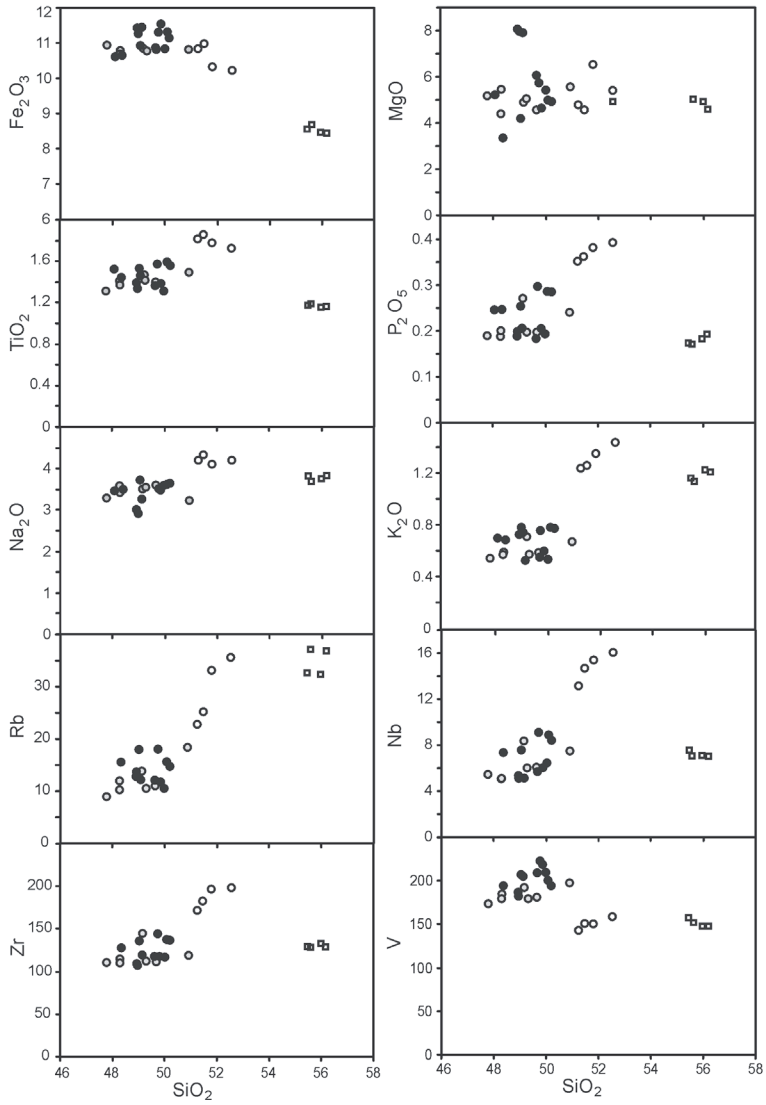

Fig. 6. Variation diagrams for selected elements. (Symbols as in Fig. 4.)

fractionation process during the ascent of magmas. Olivine and clinopyroxene are the dominant fractionating phases. Plagoclase+Fe-Ti oxides may also have been important fractionated phases.

Crustal contamination

Because the Karasar basalt was extruded through the continental crust, it is essential to evaluate the possible effects of crustal contamination before consideration the nature of mantle sources and melting processes. The extent of wall rock contamination in continental basalts is controversial and difficult to identify unless chemical compositions of both contaminant and magmatic source are independently known (Carlson & Hart 1988). Contamination by crustal rocks could mainly increase the abundances of highly incompatible elements in basaltic melts, but it has little effect on the contents of heavy rare earth elements (HREE) and high-field strength elements (HFSE, e.g. Nb, Ti and Ta) due to low concentrations of these elements in the crust (Taylor & McLennan 1985). Highly incompatible trace element abundances and light-REE enrichments, which are seen in normalized diagrams (Fig. 7), may either be a consequence of crustal contamination or varying degrees of partial melting in the mantle source. In general, the addition of crustal material to basaltic magmas or their source region is expected to result in increasing of SiO_2, Rb/Sr and K_2O/P_2O_5 (Carlson & Hart 1988), although this relationship may be complicated by assimilation–fractional crystallization and partial melting effects (DePaolo 1981). In addition, crustal involvement results in increasing Rb/Sr and K_2O/P_2O_5 relative to Ti/Zr (Hoang & Flower 1998; Hoang & Uto 2003). Plots of Ti/Zr against Rb/Sr and K_2O/P_2O_5 for Karasar basalt samples (Fig. 9a,b) shown in relation to MORB, OIB, PM and continental crust show that the samples cluster around a narrow range of Rb/Sr (0.02–0.06) and K_2O/P_2O_5 (2.71–3.63), although quartz xenocryst-bearing rocks have higher values of Rb/Sr (0.9–0.10) and K_2O/P_2O_5 (6.21–6.67). On the other hand, continental crust generally characterized by Zr/Nb > 10 ratios and high Ce/Y ratios (e.g. Taylor & McLennan 1985). The Karasar basalt samples form a trend changing between OIB and MORB ratios, although quartz-bearing rocks slightly differ from the others (Fig. 9c). The quartz xenocryst-bearing rocks of the Karasar basalt are actually displaced away from the main array of data (Fig. 9c). Furthermore, contamination of the melts with continental crust should result in negative correlations between Nb/La and La/Sm_N which are not observed excluding quartz-bearing rocks (Fig. 9d).

In summary, it can be postulated that the Karasar basalt samples show a minimal or no effect of the crustal material, although the quartz-bearing rocks show some evidence of the crustal material.

The source of the magmas: lithospheric or asthenospheric mantle?

During the extension of the lithosphere, deeper parts of the mantle ascend and melt adiabatically (McKenzie & Bickle 1988), thus both deep lithospheric mantle and the asthenosphere are possible magma sources. Karasar basalt exhibits trace element ratios, which strongly differ from those of oceanic basalts (OIB and MORB, Fig. 10), as is the case of many continental flood basalts (CFBs) and volcanic arc basalts. Most of these CFBs have been interpreted as subcontinental lithospheric mantle derived melts (Lightfoot et al. 1993; Frey et al. 1996). The subcontinental lithospheric mantle is often modified by fluids related to dehydration in subduction zones (Noll et al. 1996; Brenan et al. 1996) and may have incorporated subducted sediments (Ben Othman et al. 1989; Sun & McDunough 1989). These processes induce relative depletions in Ti, Nb, and Ta and relative enrichments in Ba resulting in negative Nb-Ta anomalies on the normalized trace ele-

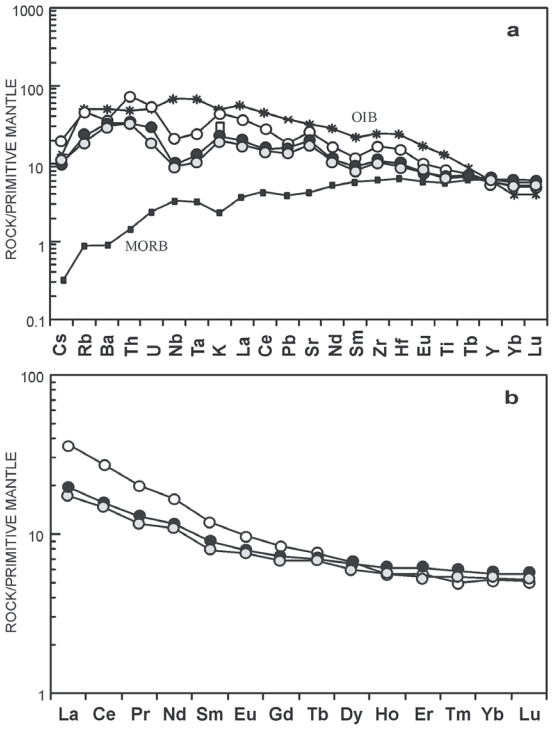

Fig. 7. Primitive mantle normalized diagrams for Karasar basalt. **a** — Trace elements (normalized values from Sun & McDunough 1989); **b** — Rare earth elements. (Normalized values from Sun 1982; symbols as in Fig. 4.)

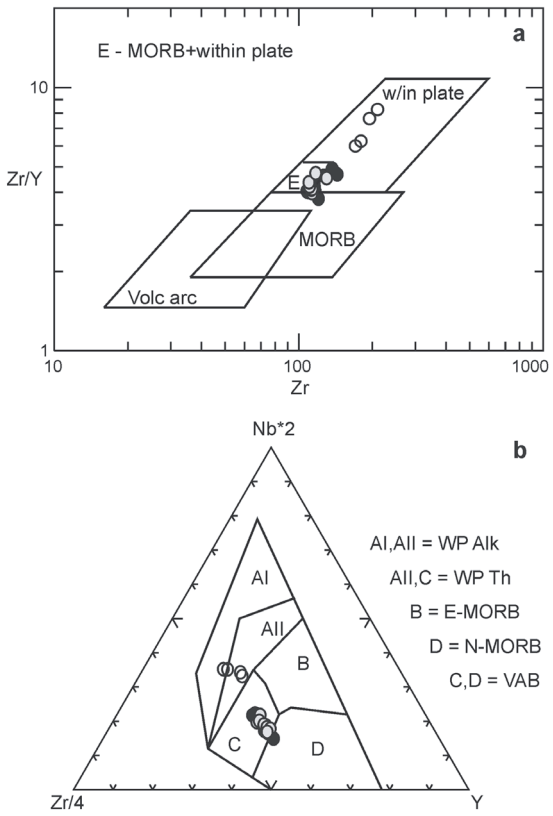

Fig. 8. Geotectonic discrimination plots for the Karasar basalts. **a** — Zr/Y-Zr diagram of Pearce & Cann 1973; **b** — Nb-Zr-Y diagram of Meschede 1986. (Symbols as in Fig. 4.)

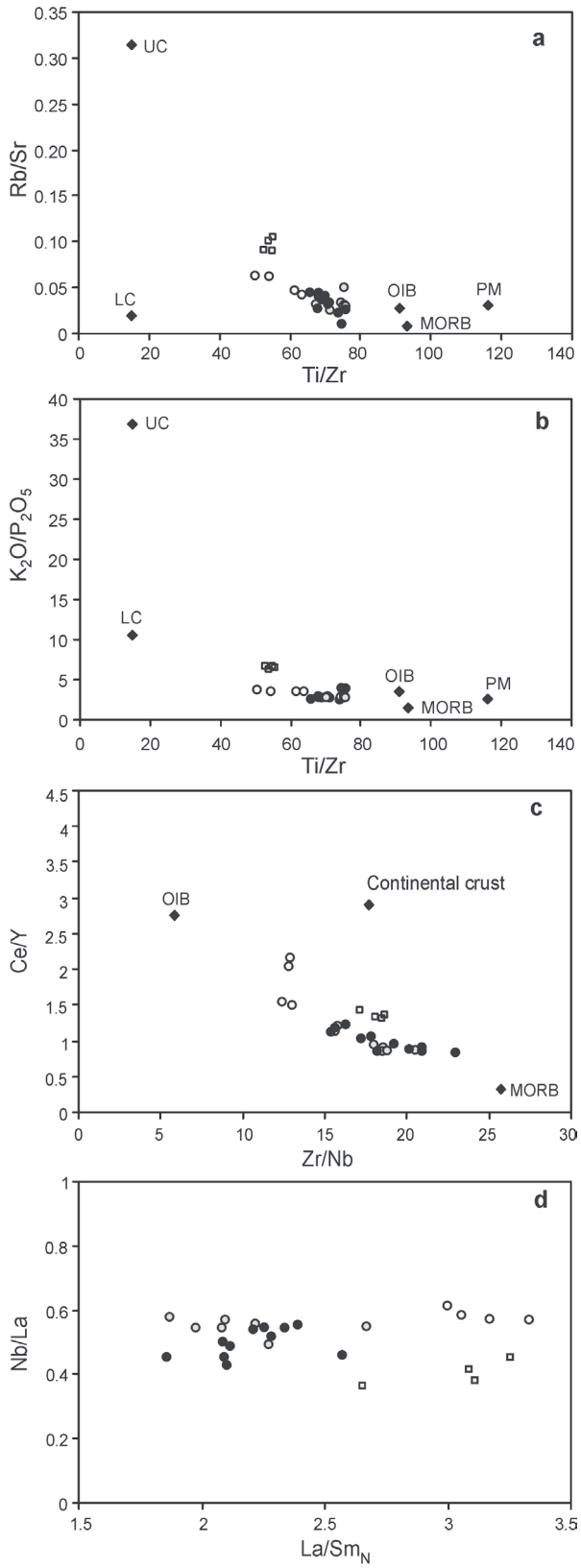

Fig. 9. **a** — Ti/Zr-Rb/Sr, **b** — K_2O/P_2O_5-Ti/Zr, **c** — Zr/Nb-Ce/Y, **d** — La/Sm_N-Nb/La diagrams for the Karasar basalt. (MORB, OIB and PM after Sun & McDunough 1989; LC — lower crust, UC — upper crust and AC — average crust after Taylor & McLennan 1985. Symbols as in Fig. 4.)

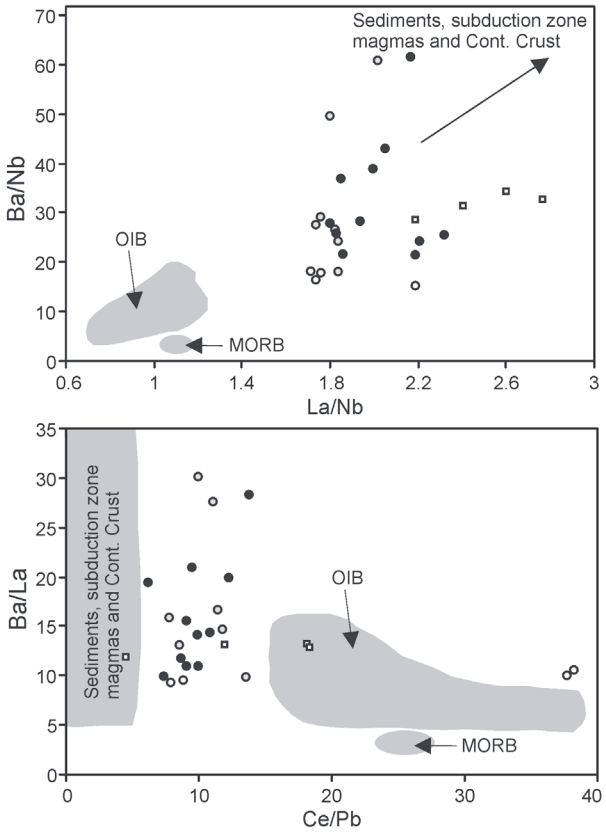

Fig. 10. Selected trace element ratios diagrams for the Karasar basalt. The fields of OIB, MORB, sediments, and subduction zone magmas are from Weaver (1991), Sun & McDunough (1989), and Ben Othman et al. (1989). (Symbols as in Fig. 4.)

ment patterns. It has been proposed that negative Nb-Ta anomalies in the intra-continental basalts reflect a subcontinental lithospheric mantle source (e.g. Arndt et al. 1993; Turner & Hawkesworth 1995). La/Nb ratio can be used to discriminate between asthenospheric and lithospheric mantle sources. Subcontinental lithospheric mantle sources typically have La/Nb>1 whereas asthenospheric melts have La/Nb<1 (Fitton et al. 1991). All samples of the Karasar basalt have La/Nb>1 implying their lithospheric signature. However, some authors (Kelemen et al. 1990; Arndt & Christensen 1992) have proposed that the relative depletion of HFSE, especially Nb and Ta, in continental lavas, could result from interactions between the subcontinental lithospheric mantle and asthenospheric melt. The correlations observed between trace element ratios (Fig. 10) indicate that the lithospheric signature of the Karasar basalt cannot simply result from relative element depletions due to crystallization of HFSE-bearing-oxides during the transit and percolation of asthenospheric magmas through the lithospheric mantle. Considering these characteristics, it can be concluded that the source of the Karasar basalt is likely to be as lithospheric rather than asthenospheric mantle.

Mantle source characteristics

All types of the Karasar basalt are characterized by a depletion of Nb-Ta on the primitive mantle normalized diagram (Fig. 7a). The large trough at Nb-Ta could reflect the existence of a residual Nb-Ta bearing phase in the source during the partial melting, which has been explained in terms of retention of this element in the source during partial melting (Pearce 1996), by the effects of crustal contamination (Cox & Hawkesworth 1985), or by the presence of subduction modified mantle (Peate et al. 1997). Rock samples have been plotted on the Th/Yb-Nb/Yb diagram (Fig. 11a) modified from Pearce (1983). These ratios are independent of fractional crystallization and/or partial melting, and thus indicate source variations. Basaltic magmas from mantle asthenosphere or plume asthenosphere, all lie within or close to a diagonal mantle array defined by Th/Nb ratios. However, source region metasomatism by subduction processes results in enrichment of Th with respect to Nb and hence Th/Yb ratios higher than Nb/Yb, as subduction components generally carry Th but not Nb or Yb. Figure 11a shows that all samples are displaced to high Th/Yb ratios relative to mantle array. It should be noted that the Karasar basalt samples are shifted from the mantle array forming a sub-parallel trend to that array. This can reflect a variety of processes from fractional crystallization and partial melting acting on a magma derived from a mantle containing a subduction component. Furthermore, subduction-related processes as a cause of metasomatism can readily be distinguished by HFSE and REE contents. If subduction-related metasomatism was involved, one would expect a systematic depletion of HFSE (e.g. Ta and Hf) relative to REE (e.g. La and Sm), because REE are much more soluble than HFSE in fluids (Jones et al. 1995). Considering the low HFSE/REE ratios of the Karasar basalt, subduction-related metasomatism appears as a more suitable enrichment process (Fig. 11b). In addition, K/Nb ratios of the basaltic samples range between 711–1243 compared to a value of 250 for average depleted MORB (Hoffmann 1988) implying a relative enrichment in K. An addition of these elements by partial melting processes appears unlikely because melting processes of spinel or garnet peridotite do not fractionate these elements from another or other highly incompatible elements (Haase et al. 2000). Fluid metasomatism of continental lithospheric mantle (Hawkesworth et al. 1986) is a possible mechanism to produce the enrichment of the alkaline and alkaline earth elements. This mechanism also explains the observed patterns of the Karasar basalt in the trace element patterns in Fig. 7a.

Partial melting in mantle

Varying concentrations of trace and rare earth elements in the basaltic provinces can be explained by varying degrees of partial melting of a single mantle source, derivation from different mantle sources and various degrees of fractionation (Clague & Frey 1982; Hofmann et al. 1984; Wilson 1989; Thomas et al. 1999). Low degrees of partial melting could produce the enriched basaltic melts from a mantle source, while high degrees of partial melting could generate the basaltic melts with lower concentrations of incompatible trace elements. All types of the Karasar basalt show patterns characterized by variable enrichments degrees relative to primitive mantle concentrations in normalized trace and rare element patterns (Fig. 7). The REE patterns indicate some differences

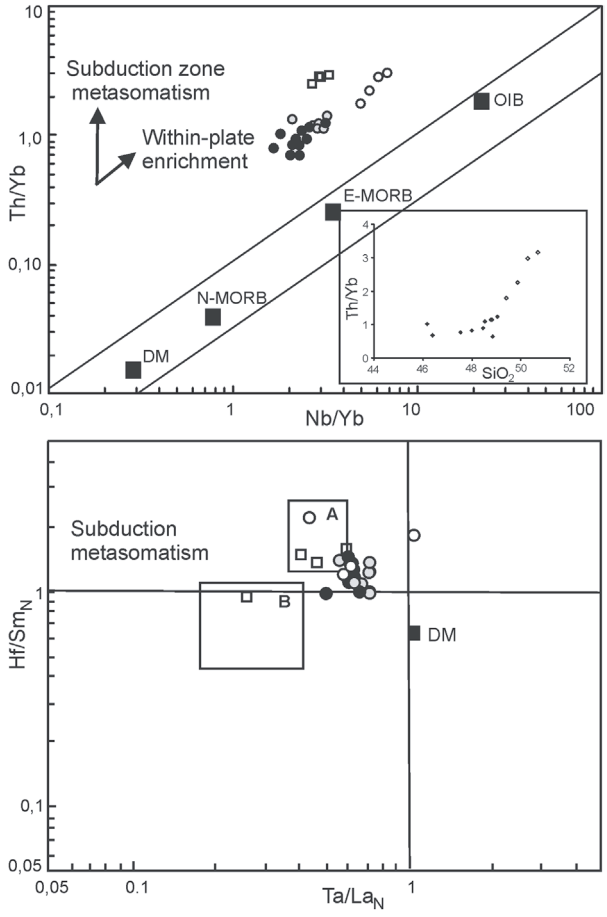

Fig. 11. a — Th/Yb-Nb/Yb diagram (after Pearce 1983) for the Karasar basalt. All samples exhibit a consistent displacement from the mantle array indicating subduction-related metasomatism and/or crustal contamination. **b** — Hf/Sm_N and Ta/La_N diagram. All samples show the characteristic depletion of Ta relative to La observed in basalts produced by mantle source metasomatized by subduction related processes. Fields A and B: volcanic arc basalts taken from Yogodzinski et al. (1995) and Francalanci et al. (1993), respectively. (Depleted mantle (DM), normal-type MORB (N-MORB), enriched MORB (E-MORB) and ocean island basalts (OIB) after Sun & McDunough 1989.)

between these basalts. Trachybasalt has steeper slope than the other basalts in LREE. In general, primitive mantle normalized REE patterns for the ne-normative basalt and trachybasalt show a slight depletion in HREE relative to primitive mantle values. These convex-downward patterns are characterized by enrichments in LREE. Hy-normative tholeiites also contain higher concentrations of medium-heavy rare earth elements (Fig. 7b and Table 1).

Hy-normative tholeiites have generally higher concentrations of total iron than the ne-normative basalts and trachybasalts, and trachybasalts have higher Na_2O contents than the others indicative of increasing melting pressure (i.e. depth) coupled with decreasing degree of melting (SiO_2). Na_2O, TiO_2 and K_2O are moderately incompatible in mantle peridotite and are concentrated in small melt fractions; as such their concentrations in a melt decrease as the degree of melting (SiO_2) increases (Klein & Langmuir 1987). The trachybasalts of the Karasar basalt have higher concentrations of these elements suggesting different melting supporting evidence that volcanism in this region is the result of partial melting rather than changing composition of the mantle source.

Rare earth element ratios are useful for constraining the extent of partial melting along with the mineralogy and chemistry of the source. This is because the solid/melt partitioning is different for spinel and garnet peridotite sources. Partial melting of either a garnet or spinel peridotite will prefentially enrich the LREE in the melt and produce La/Yb variations with variable degrees of partial melting, although the La/Yb variations will be much larger for melting of garnet peridotite source than of spinel peridotite source (Shaw et al. 2003). In addition, the degree of enrichment of MREE relative to HREE depends on whether garnet exists as a residual phase during melting, as HREE are prefentially retained by garnet during partial melting relative to MREE (e.g using distribution coefficients from McKenzie & O'Nions 1991).

In the light of the above, a more useful approach to melt modeling is the use of plots of LREE/HREE vs. MREE/HREE ratios, e.g. La/Yb and Dy/Yb. These plots are particularly useful as they distinguish between melting in the spinel and garnet peridotite sources (Thirwall et al. 1994; Baker et al. 1997). Spinel-peridotite melting produces little change in Dy/Yb ratios in melts compared with their mantle source and there is also little change in Dy/Yb ratio of the Karasar basalt (Fig. 12). In contrast, garnet-peridotite melting produces large changes in Dy/Yb ratios. A second feature of such plots is that mixing between different melt fractions will generate linear mixing arrays.

Modelling of La/Yb and Dy/Yb ratios, coupled with Yb abundances, is presented in Fig. 12. These plots show the Dy/Yb_N vs. La/Yb_N data for the Karasar basalt data set along with trajectories for non-modal fractional melts of garnet and spinel-peridotite sources. The source concentrations use primitive mantle values from Taylor & McLennan (1985), which is a crude starting approximation of the likely source concentrations. The following points can be gleaned from those models:

1. A depleted MORB mantle source does not have La/Yb ratios high enough to reproduce the La/Yb ratios of most samples of the Karasar basalt (Fig. 12a). Primitive mantle normalized diagram also implies a source more enriched than MORB mantle.

2. Variable degrees of partial melting of a garnet-peridotite source cannot generate the observed co-variation in Dy/Yb_N ratio with changing La/Yb_N ratio (Fig. 12b,c). Melting of a garnet peridotite should produce melts with much higher La/Yb_N ratios than the Karasar basalt samples at reasonable degrees of partial melting, so that the lowest Dy/Yb_N ratios of dataset require unrealistically large degrees of melting of garnet peridotite source (>25 %). In addition, melting a garnet peridotite source should produce melts exhibiting no co-variation between La/Yb_N and Yb_N (Fig. 12c) as Yb retained by garnet in the source.

3. The Karasar basalt samples show small but significant co-variation between La/Yb-and Yb, which suggests melting involved a spinel peridotite source, although trachybasalt samples of the Karasar basalt form a linear array toward the garnet peridotite melting trajectory (Fig. 12c).

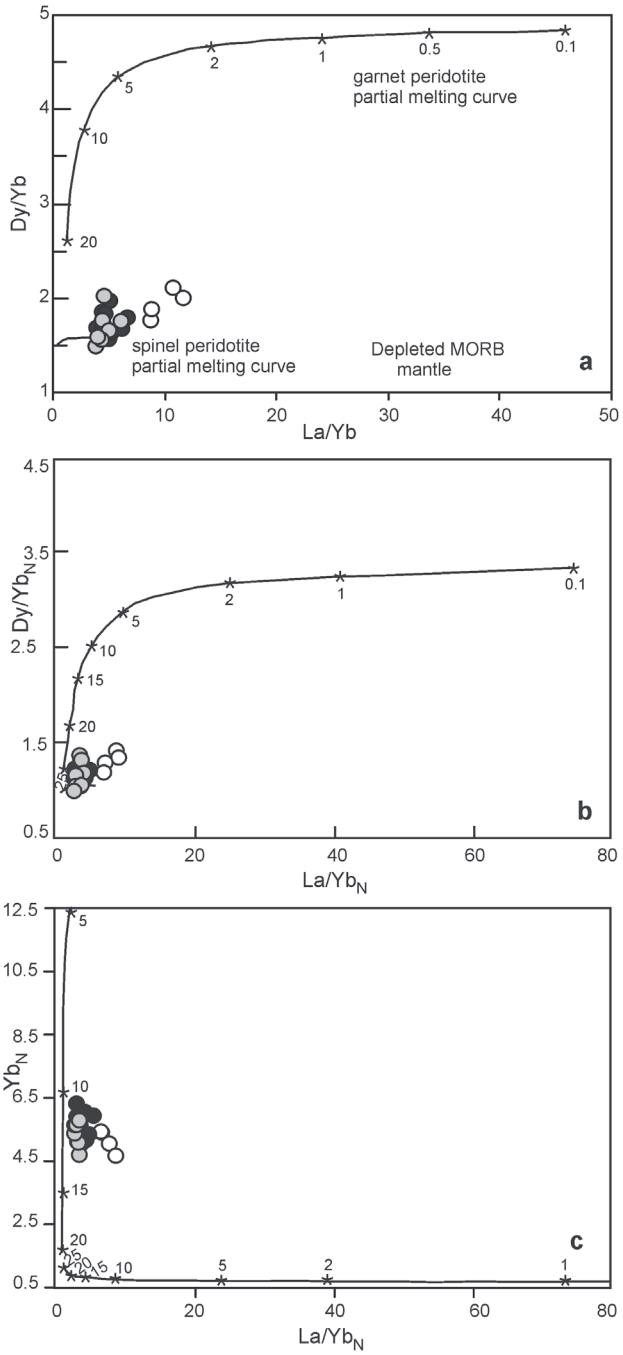

Fig. 12. La/Yb vs. Dy/Yb and Yb. Melt curves are point-average, non-modal fractional melts of garnet and spinel lherzolites (garnet lherzolite: 0.598 ol, 0.211 opx, 0.076 cpx, 0.115 gt which melts in the proportions 0.05 ol, 0.20 opx, 0.30 cpx, 0.45 gt; spinel lherzolite: 0.578 ol, 0.270 opx, 0.119 cpx, 0.033 sp which melts in the proportions 0.10 ol, 0.27 opx, 0.50 cpx, 0.13 sp; Thirlwall et al. 1994). Source compositions of depleted MORB, primitive mantle and distribution coeficients were taken from Taylor & McLennan 1985 and McKenzie & O'Nions (1991), respectively.

The simplest model to account for the REE systematics of the Karasar basalt samples involves mixing of small melt fractions from garnet peridotite source with relatively larger melt fractions from spinel peridotite source (Fig. 12b).

In summary, melting extended in depth ranging from spinel peridotite to garnet peridotite. For example, most samples including hyperstene-normative and nepheline-normative basalts appear to be derived from spinel-peridotite source whereas trachybasalts require a mixing between a melt with a larger degree of partial melting in a spinel-peridotite source and a melt with a small degree of partial melting in a garnet-peridotite source. This approximation also explains enrichments in LREE and depletions in HREE for alkaline samples relative to tholeiitic samples of the Karasar basalt.

Conclusions

1. The Karasar basalt mainly comprises the hyperstene-normative, nepheline-normative basalts, trachybasalts (hawaiites) and quartz-bearing basaltic andesites. Quartz-bearing rocks, which form the lowermost part of the Karasar basalt, obtained from drilling core samples characterized by high silica contents, varying from 54.34–55.07 % SiO_2, high Rb, Th, U, Cs and light rare earth element concentrations (Table 1) relative to basaltic samples.

2. All samples of the Karasar basalt have variable enrichments in LILE and LREE in primitive mantle normalized trace element patterns and characterized by negative anomalies at Nb-Ta. The hy-normative tholeiites have higher concentrations of HREE relative to the ne-normative basalts and trachybasalts, whereas the trachybasalts have higher concentrations of LREE resulting steeper slope in normalized REE pattern relative to other basalts.

3. The Karasar basalt also shares several common compositional trends. The most robust of these is an overall increase in incompatible trace element concentrations from the hy- and ne-normative basalts to the trachybasalts (Fig. 7). Increases of greater magnitude are generally associated with highly incompatible elements (for Th, La, Rb, K, Zr, Nb etc.) and ratios of highly to moderately incompatible elements (e.g. Ce/Y and Zr/Y). There are also common compositional trends in some of the major elements. Similarly, other highly incompatible elements, both K_2O and P_2O_5 show a clear, large magnitude increase from the hy- and ne-normative basalts to the trachybasalts. TiO_2 and SiO_2 (except quartz-bearing samples) also increase in same manner.

4. The trace element characteristics of the Karasar basalt imply that the crustal effects on the magmas have minimal or no effect, but quartz-bearing samples have some influences of crustal material.

5. Varying concentrations of the incompatible trace and rare earth elements contents seen in primitive mantle normalized diagrams suggest that the Karasar basalt can be explained by varying degrees of partial melting in a single mantle source. REE modeling indicates that the magmas forming the Karasar basalt derived from a spinel-peridotite source, although trachybasalts require an interaction between melts with larger degree of partial melting in spinel-peridotite and melts with lower degree of partial melting in garnet peridotite source.

6. The Karasar basalt was most likely derived from a metasomatized mantle source due to decompressional partial melting as the overlying continental crust was ruptured and

thinned as a result of the lateral escape of the Anatolian plates along both the east Anatolian and north Anatolian faults and related secondary strike-slip fault systems during the post-collisional extensional tectonic regime following the collision between the Eurasian and Arabian plates. Volcanism in this part of Anatolia is consistent with a model in which melting of lithospheric mantle occurred in response to lithospheric extension.

Acknowledgments: This study was supported with a project numbered as M-182 by the Cumhuriyet University Research Foundation (CURF, Sivas-Turkey). We thank the CURF for its supporting. We also thank the MTA for its logistical supporting during the field study.

References

Alpaslan M. & Terzioğlu N. 1996: Comparative geochemical features of the Upper Miocene and Pliocene volcanics in the Arguvan area (N-Malatya), Turkey. *Geol. Bull. Turkey* 39, 75–86.

Arndt N.T. & Christensen U. 1992: The role of lithospheric mantle in continental flood volcanism: Thermal and geochemical constraints. *J. Geophys. Res.* 97, 10967–10981.

Arndt N.T., Czamanske G.K., Wooden J.L. & Foderenko V.A. 1993: Mantle and crustal contributions to continental flood volcanism. *Tectonophysics* 223, 39–52.

Baker J., Thirwall M. & Menzies M. 1996: Sr-Nd-Pb isotopic and trace element evidence for crustal contamination of plume-derived flood basalts: Oligocene flood volcanism in Western Yemen. *Geochim. Cosmochim. Acta* 60, 2559–2581.

Ben Othman D., White W.M. & Patchett J. 1989: The geochemistry of marine sediments, island arc magma genesis, and crust-mantle recycling. *Earth Planet. Sci. Lett.* 94, 1–21.

Brenan J.M., Shaw H.F., Ryerson F.J. & Phinney D.L. 1995: Mineral-aqueous fluid partitioning of trace elements at 900 °C and 2.0 GPa: Constraints on the trace chemistry of mantle and deep crustal fluids. *Geochim. Cosmochim. Acta* 59, 3331–3350.

Bozkurt E. 2001: Neotectonics of Turkey — a synthesis. *Geodynamica Acta* 14, 3–30.

Buket E. & Temel A. 1998: Major element, trace element, and Sr-Nd isotopic geochemistry and genesis of Varto (Muş) volcanic rocks, Eastern Turkey. *J. Volcan. Geotherm. Res.* 85, 405–422.

Carlson R.W. & Hart W.K. 1988: Flood basalt volcanism in the northwestern United States. In: MacDougall J.D. (Ed.): Continental flood basalts. *Kluwer Academic Publishing*, 63–110.

Clague D.A. & Frey F.A. 1982: Petrology and trace element geochemistry of the Honolulu volcanics, Oahu: implications for the oceanic mantle below Hawaii. *J. Petrology* 23, 447–504.

Coffin M.F. & Eldholm O. 1992: Volcanism and continental breakup: a global compilation of large igneous provinces. In: Storey B.C., Alabaster T. & Pankhurst R.J. (Eds.): Magmatism and the causes of continental break-up. *Geol. Soc. London, Spec. Publ.* 68, 21–34.

Cox K.G. & Hawkesworth C.J. 1985: Geochemical stratigraphy of the Deccan Traps, at Mahabaleshwar, Western Ghats, India, with imlications for open system magmatic processes. *J. Petrology* 26, 355–377.

DePaolo D.J. 1981: Trace element and isotopic effects of combined wallrock assimilation and fractional crystallization. *Earth Planet. Sci. Lett.* 53, 189–202.

Ekici T. 2003: Petrology of the Neogene volcanics along the Malatya fault between Arguvan and Arapkir (Malatya). *Ph.D. Thesis,* Çukurova University, 1–121 (unpublished).

Fitton J.G., James D., Kempton P.D., Ormerod D.S. & Leeman W.P. 1988: The role of lithospheric mantle in the generation of late-Cenosoic basic magmas in the Western United States. *J. Petrology,* Spec. Lithosphere Issue, 331–349.

Fitton J.G., James D. & Leeman W.S. 1991: Basic magmatism associated with late Cenozoic extension in the western United States: compositional variations in space and time. *J. Geophys. Res.* 96, 13693–13711.

Fram M.S. & Lesher C.E. 1997: Generation and polybaric differentiation of East Greenland early Tertiary flood basalts. *J. Petrology* 38, 231–275.

Francalanci L., Taylor S.R., McCulloch M.T. & Woodhead J.D. 1993: Geochemical and isotopic variations in the calc-alkaline rocks of Aeolian arc, southern Tyrrhenian Sea, Italy: constraints on magma genesis. *Contr. Mineral. Petrology* 113, 300–313.

Frey F.A., McNaughton N.J., Nelson D.R., deLaeter J.R. & Duncan R.A. 1996: Petrogenesis of the Bunbury basalt, western Australia: Interaction between the Kerguelen plume and Gondwana lithosphere? *Earth Planet. Sci. Lett. 144*, 163–183.

Gill J.B. 1981: Orogenic andesites and plate tectonics. *Springer-Verlag,* New York, 1–389.

Gülen L. 1984: Sr, Nd, Pb isotope and trace element geochemistry of calc-alkaline and alkaline volcanics, eastern Turkey. *Ph.D. Thesis, Massachusetts Inst. Technology,* USA, 1–232 (unpublished).

Gültekin A.S. 1993: Geology of the area between Alacahan-Çetinkaya-Divriği (Sivas), *PhD. Thesis,* İstanbul Univ., 1–180 (unpublished).

Haase K.M., Muhe R. & Stoffers P. 2003: Magmatism during extension of the lithosphere: geochemical constraints from lavas of the Shaban Deep, northern Red Sea. *Chem. Geol.* 166, 225–239.

Hart S.R. 1984: A large scale isotope anomaly in the southern-hemisphere mantle. *Nature* 309, 753–757.

Hawkesworth C.J., Norry M.J., Roddick J.C. & Vollmer R. 1979: $^{143}Nd/^{144}Nd$ and $^{87}Sr/^{86}Sr$ ratios from the Azores and their significance in LIL-element enriched mantle. *Nature* 280, 28–31.

Hawkesworth C.J., Rogers N.W., Calsteren P.W.C. & Menzies M.A. 1984: Mantle enrichment processes. *Nature* 311, 331–335.

Hawkesworth C.J., Mantovani M.S.M., Taylor P.N.E. & Palacz Z. 1986: Evidence for the Parana of South Brazil for a continental contribution to Dupal basalts. *Nature* 322, 356–359.

Heming R.F. 1980: Petrology and geochemistry of Quaternary basalts from Northland, New Zealand. *R. Soc. N.Z. Bull.* 23, 64–75.

Hempton M.R. 1987: Contsraints on Arabian plate motion and extensional history of the Red Sea. *Tectonics* 6, 687–705.

Hoang N. & Flower M.F.J. 1998: Petrogenesis of Cenozoic basalts from Vietnam: implication for origins of a "diffuse igneous province". *J. Petrology* 39, 369–395.

Hoang N. & Uto K. 2003: Origin of mantle isotopic components beneath southwest Japan. *Chem. Geol.* 198, 3–4, 249–268.

Hofmann A.W. 1988: Chemical differentiation of the Earth: the relationship between mantle, continental crust, and oceanic crust. *Earth Planet. Sci. Lett.* 90, 297–314.

Hofmann A.W., Feigenson M.D. & Razcek I. 1984: Case studies on the origin of basalt. III. Petrogenesis of the Mauna Ulu eruption, Kilauea, 1969–1971. *Contr. Mineral. Petrology* 88, 24–35.

Innocenti F., Mazzuoli R., Pasquare G., Radication di Brozolo F. & Villary L. 1976: Evolution of volcanism in the area of interaction between the Arabian, Anatolian and Iranian plates (Lake Van, Eastern Turkey). *J. Volcanol. Geotherm. Res.* 1, 103–112.

Irvine T.N. & Baragar W.R.A. 1971: A guide to the geochemical classification of the common volcanic rocks. *Canad. J. Earth Sci.* 8, 523–548.

Jahn B.M. & Zhang Z.Q. 1984: Archaean granulite gneisses from eastern Hebei province, China: rare earth geochemistry and

tectonic implications. *Contr. Mineral. Petrology* 85, 224–243.

Jones J.H., Walker D., Pickett D.A., Murrell M.T. & Beattie P. 1995: Experimental investigations of the partitioning of Nb, Mo, Ba, Ce, Pb, Ra, Th, Pa, and U between immiscible carbonate and silicate liquids. *Geochim. Cosmochim. Acta* 59,1307–1320.

Kelemen P.B., Johnson K.T.M., Kinzler R. & Irving A.J. 1990: High field strength element depletion in arc basalts due to mantle-magma interaction. *Nature* 345, 521–524.

Keskin M., Pearce J.A. & Mitchell J.G. 1998: Volcano-stratigraphy and geochemistry of collision-related volcanism on the Erzurum-Kars Plateau, northeastern Turkey. *J. Volcanol. Geotherm. Res.* 85, 1–4, 355–404.

Klein E.M. & Langmuir C.H. 1987: Global correlations of oceanic ridge basalt chemistry with axial depth and crustal thickness. *J. Geophys. Res.* 92, 8089–8115.

Koçyiğit A., Yılmaz A., Adamia S. & Kuloshvili S. 2001: Neotectonics of East Anatolian Plateau (Turkey) and Lesser Caucasus: implication for transition from thrusting to strike-slip faulting. *Geodinamica Acta* 14, 177–195.

Lambert R.S.J., Holland J.G. & Owen P.F. 1974: Chemical petrology of a suite of calc-alkaline lavas from Mt. Ararat, Turkey. *J. Geology* 82, 419–438.

Le Maitre R.W. 1989: A classification of igneous rocks and glossary of terms. *Blackwell Sci. Publ.,* Oxford, 1–193.

Le Roux A.P. 1986: Geochemical correlation between southern African kimberlites and South Atlantic hotspots. *Nature* 324, 243–245.

Lightfoot P.C., Hawkesworth C.J., Hergt J., Naldrett A.J., Gorbatchev N.S., Fedorenko V.A. & Doherty W. 1993: Remobilisation of the continental lithosphere by a mantle plume: Major-, trace-element, and Sr-, Nd-, and Pb-isotope evidence from picritic and tholeiitic lavas of the Noril'sk District, Siberian Traps, Russia. *Contr. Mineral. Petrology* 114, 171–188.

McDunough W.F. 1990: Constraints on the compositions of the continental lithospheric mantle. *Earth Planet. Sci. Lett.* 101, 1–18.

McDunough W.F., McCullogh M.T. & Sun S.S. 1985: Isotopic and geochemical systematics in Tertiary-recent basalts from southeastern Australia and implications for the evolution of the subcontinental lithosphere. *Geochim. Cosmochim. Acta* 49, 2051–2067.

McKenzie D.P. 1969: Plate tectonics of the Mediterranean region. *Nature* 220, 239–343.

McKenzie D.P. 1972: Active tectonics of the Mediterranean region. *Geophys. J. Royal Astron. Soc.* 30, 109–185.

McKenzie D.P. & Bickle M.J. 1988: The volume and composition of melt generated by extension of the lithosphere. *J. Petrology* 29, 625–679.

McKenzie D.P. & O'Nions R.K. 1991: Partial melt distribution from inversion of rare earth element concentrations. *J. Petrology* 32, 1021–1091.

Meschede M. 1986: A method of discriminating between different types of mid-ocean ridge basalts and continental tholeiites with the Nb-Zr-Y diagram. *Chem. Geol.* 56, 207–218.

Noll P.D., Newsom H.E., Leeman W.P. & Ryan J.G. 1996: The role of hydrothermal fluids in the production of subduction zones magmas: Evidence from siderophile and chalcophile trace elements and boron. *Geochim. Cosmochim. Acta*. 60, 587–611.

Özgül N., Turşucu A., Özyardımcı N., Şenol M., Bingöl İ. & Uysal Ş. 1981: Geology of the Munzur Mountains. *MTA Report, Rep. Num*. 6995, Ankara (unpublished).

Pearce J.A. 1983: Role of sub-continental lithosphere in magma genesis at destructive plate margins. In: Hawkesworth C.J. & Norry M.J. (Eds.): Continental basalts and mantle xenoliths. *Nantwich,* Shiva, 230–249.

Pearce J.A. 1996: Sources and settings of granitic rocks. *Episodes* 19, 120–125.

Pearce J.A. & Cann J.R. 1973: Tectonic setting of basic volcanic rocks determined using trace element analyses. *Earth Planet. Sci. Lett.* 19, 290–300.

Pearce J.A., Bender J.F., DeLong S.E., Kidd W.S.F., Low P.J., Güney Y., Şaroğlu F., Moorbath S. & Mitchell J.G. 1990: Genesis of collisional volcanism in Eastern Anatolia, Turkey. In: LeFort P., Pearce J.A. & Pecher A. (Eds.): Collisional magmatism. *J. Volcanol. Geotherm. Res.* 44, 184–229.

Peate D.W., Pearce J.A., Hawkesworth C.J., Colley H., Edwards C.M.H. & Hirose K. 1997: Geochemical variations in Vanuatu arc lavas: The role of subducted material and variable mantle wedge composition. *J. Petrology* 38, 1331–1358.

Reiners P.W. 2002: Temporal-compositional trends in intraplate basalt eruptions: Implications for mantle heterogeneity and melting processes. *Geochemistry, Geophysics, Geosystems (G^3)* 3, 1–30.

Saunders A.D., Storey M., Kent R.W. & Norry M.J. 1992: Consequences of plume-lithosphere interactions. In: Storey B.C., Alabaster J. & Pankhurst R.J. (Eds.): Magmatism and the causes of continental break-up. *Geol. Soc. London, Spec. Publ.* 68, 41–60.

Saunders A.D., Larsen H.C. & Fitton J.G. 1998: Magmatic development of the southeast Greenland margin and the evolution of the Iceland plume: Geochemical constraints from Leg 152. In: Saunders A.D., Larsen H.C. & Wise S.H. (Eds.): *Proc. ODP, Sci. Results,* 152: College Station, TX (Ocean Drilling Program), 479–501.

Shaw E.J., Baker A.J., Menzies M.A., Thirwall M.F. & Ibrahim M.K. 2003: Petrogenesis of the largest intraplate volcanic field on the Arabian plate (Jordan): A mixed lithosphere-asthenosphere source activated by lithospheric extension. *J. Petrology* 44, 9, 1657–1679.

Sun S.S. 1982: Chemical composition and origin of the Earth's primitive mantle. *Geochim. Cosmochim. Acta* 46, 179–192.

Sun S.S. & McDunough W.F. 1989: Chemical and isotopic systematics of oceanic basalts: implications for mantle composition and processes. In: Saunders A.D. & Norry M.J. (Eds.): Magmatism in ocean basins. *Geol. Soc. London, Spec. Publ.* 42, 313–345.

Şaroğlu F. & Yılmaz Y. 1984: Neotectonics of the Eastern Anatolia and related magmatism. In: Ketin Symposium, Proceeding. *Geol. Soc. Turkey,* Ankara, 149–162.

Şengör A.M.C. 1980: Fundementals of the neotectonic of Turkey. *Geol. Soc. Turkey,* Ankara, 1–40.

Şengör A.M.C. & Kidd W.S.F. 1979: Post-collisional tectonics of the Turkish-Iranian plateau and a comparison with Tibet. *Tectonophysics* 55, 361–376.

Şengör A.M.C. & Yılmaz Y. 1981: Tethyan evolution of Turkey: a plate tectonic approach. *Tectonophysics* 75, 181–241.

Şengör A.M.C., Görür N. & Şaroğlu F. 1985: Strike-slip faulting and related basin formation in zones of tectonic escape: Turkey as a case study. In: Biddle K.T. & Christie-Blick N. (Eds.): Strike-slip deformation, basin formation and sedimentation. *Society for Economic Paleontology and Mineralogy, Spec. Publ.* 37, 227–264.

Taylor S.R. & McLennan S.M. 1985: The continental crust: Its composition and evolution. *Blackwell,* Oxford, 1–312.

Thirwall M.F., Upton B.G.J & Jenkins C. 1994: Interaction between continental lithosphere and the Iceland plume: Sr-Nd-Pb isotope geochemistry of Tertiary basalts, NE Greenland. *J. Petrology* 35, 839–879.

Thomas L.E., Hawkesworth C.J., Van Calsteren P., Turner S.P. & Rogers N.W. 1999: Melt generation beneath ocean islands: A U-Th-Ta isotope study from Lanzarote in the Canary Islands. *Geochim. Cosmochim. Acta* 63, 4081–4099.

Thompson R.N., Morrison M.A., Dickin A.P. & Hendry G.L. 1983:

Continental flood basalts: arachnids rule OK? In: Hawkesworth C.J. & Norry M.J. (Eds.): Continental basalts and mantle xenoliths. *Nantwitch,* Shiva, 158–185.

Tokel S. 1984: Crust deformation mechanism in the East Anatolia and petrogenesis of young volcanics. In: Ketin Symposium, Proceeding. *Geol. Soc. Turkey,* Ankara, 121–130.

Turner S. & Hawkesworth C.J. 1995: The nature of the sub-continental mantle: Constraints form major-element composition of continental flood basalts. In: McDunough W.F., Arndt N. & Shirey S. (Eds.): Chemical evolution of the mantle. *Chem. Geol.* 120, 295–314.

Weaver B.L. 1991: The origin of ocean island basalts end-member compositions: trace element and isotopic constraints. *Earth Planet. Sci. Lett.* 104, 381–397.

White R.S. & McKenzie D. 1995: Mantle plumes and flood basalts. *J. Geophys. Res.* 100, 543–586.

Wilson M. 1989: Igneous petrogenesis. *Chapmann & Hall,* London, 1–466.

Wilson M. 1993: Geochemical signatures of oceanic and continental basalts: a key to mantle dynamics? *J. Geol. Soc., London* 150, 977–990.

Winter J.D. 2001: An introduction to igneous and metamorphic petrology. *Prentice Hall*, 1–697.

Wooden J.L., Czamanske G.K., Fedorenko V.A., Arndt N.T., Chauvel C., Bouse R.M., King B-S.W., Knight R.J. & Siems D.F. 1993: Isotopic and trace element constraints on mantle and crustal contributions to Siberian continental flood basalts, Noril'sk area, Siberia. *Geochim. Cosmochim. Acta* 57, 3677–3704.

Yılmaz Y., Güner Y. & Şaroğlu F. 1998: Geology of the Quaternary volcanic centres of the east Anatolia. *J. Volcanol. Geotherm. Res*. 85, 1–4, 173–210.

Yılmaz H., Yılmaz A. & Arıkal T. 2001: Geology of the Güneş Ophiolite (Divriği-Sivas). *CD of 54th Geol. Congress, Turkey*, 54–65.

Yogodzinski G.M., Kay R.W., Volynets O.N., Koloskov A.V. & Kay S.M. 1995: Magnesian andesite in the western Aleutian Komandorsky region: implications for slab melting and processes in the mantle wedge. *Geol. Soc. Amer. Bull.* 107, 505–519.

Zindler A. & Hart S. 1986: Chemical geodynamics. *Ann. Rev. Earth Planet. Sci*. 14, 493–571.